This is an accepted manuscript of an article published by Taylor & Francis in Journal of Applied Water Engineering and Research on 10 Feb 2020, available online: https://doi.org/10.1080/23249676.2020.1723446.

Optimizing the removal of nitrate by adsorption onto activated carbon using response surface methodology based on the central composite design

Nawal Taoufik [1], Abdellah Elmchaouri [1], Sophia A. Korili [2], Antonio Gil [2,*]

[1] *Université Hassan II - Casablanca, Faculté des Sciences et Techniques, Laboratoire de Chimie Physique et de Chimie Bioorganique, BP 146, 20650 Mohammedia, Morocco*

[2] *INAMAT – Science Department, Los Acebos Building, Public University of Navarra, Campus of Arrosadia, E-31006 Pamplona, Spain*

*Corresponding authors: andoni@unavarra.es

Tel : (+34) 948169602

This study sheds light on the adsorption process for the removal of nitrate ions from synthetic aqueous solutions. This contaminant pose a potential risk to the environment and can cause health effects including cancers and methemoglobinemia in infants. When the adsorption process is carried out, the effect by the several operating parameters such as initial nitrate concentration, pH, mass of activated carbon, and contact time becomes apparent. The essential process variables are optimized using response surface methodology (RSM) based on the central composite design (CCD) experiments. For this purpose 31 experimental results are required to determine the optimum conditions. The ANOVA results obtained from the RSM studies are analyzed using a second-degree polynomial equation. The study of the determination of contour plots shows the interactions among the variables of the adsorption system. The optimum conditions for the removal of nitrates is found to be: initial nitrate concentration = 15 mg/L; initial pH 4.0; mass of activated carbon= 25 mg, and contact time = 70 min. At these optimized conditions, the maximum removal of nitrates is found to be 96.59 %. The experimental values were in excellent accord with the predicted ones by the proposed RSM models. This indicates that the quadratic models can be effectively used to predict the removal efficiency of nitrate ions by adsorption process. These low-cost adsorption methods can be effectively adopted for the removal of nitrate ions from industrial effluents.

Keywords: Nitrate removal, Adsorption, Activated carbon, Response Surface Methodology, Central Composite Design.

1. *Introduction*

The discharge of contaminants is generally provided from industrial, agricultural as well as domestic wastewater. Agricultural activity, in particular, threatens the equilibrium of ecosystems by releasing a number of pollutants that seep into the aquatic environment (Sanctis et al. 2017; Aguilar et al. 2019). Nitrogen compounds, and nitrate ions particularly, are examples of its effluents (Mankiewicz-Boczek et al. 2017; Karri et al. 2018). Nitrates are accumulating in the environment and their presence in drinking water can cause a harmful effect on human health such as blue-baby syndrome in infants and stomach cancer in adults (Wongsanit et al. 2015). Nitrates are not toxic in themselves (Su et al. 2016). Under *in vivo* favourable conditions, however, they may be reduced into nitrites and nitroso compounds (nitrosamines and nitrosamides). This can cause gastrointestinal cancer, especially gastric cancer in humans (Villanueva et al. 2014; Song et al. 2015; Schullehner et al. 2017). In fact, newborns may lack oxygen because nitrites from nitrates oxidize ferrous iron (Fe^{2+}) in the hemoglobin to ferric iron (Fe^{3+}), preventing the hemoglobin from playing its crucial role in respiratory exchanges (fixation of oxygen in the lungs and release of oxygen to tissues), a disease known as methemoglobinaemia, or blue-baby disease (Golie and Upadhyayula 2017; Ahmadi et al.2017). In addition to the effects on human health, excessive level of nitrate in water can stimulate entrophication in the aquatic environment, therefore making nitrate removal from groundwater important (Li et al. 2017; Zhang et al. 2019). As result, the nitrate concentration limit in drinking water required by the World Health Organization (WHO) and the US Environmental Protection Agency (EPA) is approximately 10 mg/L (Fu et al. 2014; Uzun and Debik. 2019).

In order to overcome this issue, several processes for nitrate removal have been used and developed, such as reverse osmosis (Luo et al. 2017; Dražević et al. 2017), ion-exchange (Ansari et al. 2017), catalytic reduction (Yun et al. 2016; Torre et al. 2016; Garcia-Fernandez et al. 2018), electrodialysis (Onorato et al. 2017; Belkada et al. 2018), and biological denitrification (Zhang et al.

2014; Lu et al. 2018). However, each of above-mentioned methods presents certain limitations. Need to regenerate ion exchange resin make the process complex and non-economical (Song and Li 2019). Electrodialysis is not simple due to their sensitive working environments (Pirsaheb et al. 2016; Riveros et al. 2019). Biological denitrification is non-economical due to the side reaction and additional cost of the chemicals used (Zhang et al. 2019). The excessive consumption of energy, make reverse osmosis expensive process (Epsztein et al. 2015; Li et al. 2018). Adsorption is one other method that is simple and economically efficient for removing nitrate ions from water, due to its ease of handling, availability of a wide range of adsorbents, comfortable repair and maintenance (El Mouzdahir et al., 2007; Moreira et al., 2017). During the last years, many researchers have been directed to the development of various adsorbents for fast removal of nitrates (Satayeva et al. 2018; Fan and Zhang 2018; Gouran- Orimi et al. 2019; El Hanache et al. 2019). Activated carbon has been the extensively used material for the treatement of contaminated water because it possesses a high sorption capacity, and is characterized by a very high porosity which allows them to develop a large surface of contact with the external environment (Ghasemi et al. 2016; Piai et al. 2019). The performance of this material is closely related to their chemical surface as well as their textures (Dasgupta et al. 2018). Hanafi and Azeema (2016), for example, have reported adsorption of nitrate onto carbon adsorbent with a very large surface area up to 2800 m^2/g. Kalantary et al. (2016) show that synthetic activated carbon with magnetic nanoparticles can reduce an important amount of nitrate in water. Mazarji et al. (2017), reported applicable conditions for the modification of commercial activated carbon. These authors improve , these modifications improved the nitrate removal efficiency. Yuan et al. (2019) studied the effect of the structure of activated carbon on the adsorption of nitrate ions in aqueous solution. Mubita et al. (2019) show the importance of textural

properties on the adsorption of nitrate on carbon. Satayeva et al. (2019) evaluate the role of the surface chemistry and the pore size distribution of activated carbon for removing nitrate from water.

In the adsorption process, many operating parameters such as initial pollutant concentration, adsorbent loading, pH, temperature, and contact time influence the process efficiency. The process's efficiency may be developed by optimizing these factors (Gadekar and Ahammed 2019; Archin et al. 2019). In the classical method, optimization is usually carried out by varying a one variable while keeping all the other variables fixed at a specific set of conditions. This method is overwhelming while wide amount of variables considered and requires large number of experiments. To overcome these limitations, research is being directed towards optimization all the affecting factors by statistical techniques such as response surface methodology (RSM). The application of RSM in adsorption process can improved product yields, reduced the number of experimental trials, evaluated the relative significance of variables and their interactions, build models, reduced development time and overall costs. Acharya et al. (2017) applied RSM to optimize the removal nitrates ions from a synthetic solution by electrocoagulation process. Three parameters named pH, electrolysis time and current were studied. The study showed that electrolysis time and current were the most significant variables that influenced the removal of nitrate from aqueous solution and the results suggest that the regression model has a good correlation with experimental data. Sabeti et al. (2019) investigated the effect of physical parameters on the removal of nitrate and phosphate by *Chlorella Vulgaris* by Response surface methodology (RSM). The results implied that the experimental values were in excellent agreement with those predicted by the proposed RSM models. Karamati-Niaragh et al. (2019) conducted the investigations to study the influence of alternating current (AC) and direct current (DC) for nitrate removal efficiency by using a continuous electrocoagulation (CEC) and designed the experiments

by response surface method. Four variables expected to affect nitrate removal were studied: initial nitrate concentration, inlet flow rate, current density and initial pH. The study clearly suggests a good accord between achieving results and the experimental data. Kuang et al. (2019) investigated the RSM to optimize the removal nitrate and its by-products by using electrochemical–adsorption (ECA) system. Three independent variables named iron particle, zeolite and current density were examined. The results showed that about 95% of initial nitrate was removed at the optimum conditions. Song et al. (2019) reported also on the investigations of the removal efficiency of nitrate and ammonia using RSM.

The main goal of this work is to optimize and model the removal of nitrate from aqueous solution using adsorption process. Central Composite Design of response surface methodology is used as a tool to evaluate the effect of the process parameters such as initial pH, nitrate concentration, contact time, and mass of activated carbon on the efficiency of nitrate removal from synthetic solution. In addition, to perform the statistical calculations, JMP software (John's Macintosh Project) is used.

2. Experimental

2.1 Materials and operating mode

Activated carbon is used as adsorbent (Hydrodalco 300, Cabot Corporation). The results of ICP analysis of activated carbon are presented in Table 1. Sodium nitrate ($NaNO_3$) from Merck was used as nitrate source.

The experimental data were collected following the completion of 31 experiments. The experimental results of all coded and actual value factors for the adsorption of nitrate on activated carbon are shown in the Table 2. In each of these experiments, we fixed, in turn, one of these

factors, namely the initial pH, initial nitrate concentration, mass of the activated carbon or contact time, and varied the other three at their levels. maximum or minimum (see Table 3).

The experimental results of all coded and actual value factors for the adsorbed quantity and the adsorption efficiency of the active carbon nitrate are also shown in the Table 3. All these experiments were carried out with 10 ml aqueous nitrate solution in 20 ml glass flasks with stirring of 280 rpm (see Figure 1). After been agitated for a predetermined time at room temperature, the suspensions were filtered through 0.45 µm Durapore membrane filters and the obtained filtrate solutions are analyzed by UV/vis spectrophotometer "Double PC (Model UVD-2950)" at the maximum absorption wavelength which was determined experimentally for nitrate (λ = 215 nm).

The removal efficiency (%) and the amount adsorbed of nitrate by solid at time (t) were calculated according to the Equations 1 and 2, respectively.

$$R_t = \left(\frac{C_0 - C_t}{C_0} \right) \times 100\% \quad \textbf{(1)}$$

$$q_t = \frac{(C_0 - C_t)V}{W} \quad \textbf{(2)}$$

where C_0 and C_t are the initial and the final concentrations of the anions in solution (mg/L), V the solution volume (L), and W is the mass of activated carbon (g).

2.2 Statistical analysis

Experimental design of the removal of NO_3^- is carried out by using the RSM. In this study, the central composite design (CCD), which is a widely exploited model of RSM, is employed to optimize the adsorption of nitrates NO_3^- onto activated carbon. Several variables affect the adsorption of these ions: initial concentration, pH, mass of activated carbon and contact time. The RSM is applied to evaluate the variables' effect on the process and to determine the relationship between a set of these controllable experimental parameters. As such, RSM is an empirical modelling technique whereby, the main aim is to organize at best the tests that accompany scientific research or industrial studies.

The actual design experiment is listed in Table 2. The low, middle, and high levels of each variable are designated as -2 (-α) and +2 (-α).

Mathematical model

The first step in RSM is to find a suitable approximation for the true functional relationship between the response $\hat{\eta}$ and the set of independent variables.

The behaviour of the system is explained by the following second-degree polynomial formula:

$$\hat{\eta} = ß_0 + \sum_{j=1}^{4} ß_j X_j + \sum_{j=1}^{4} \sum_{j'=1\ j'\neq j}^{4} ß_{jj'} X_j X_{j'} + \sum_{j=1}^{4} ß_{jj} X_j^2 \quad \textbf{(3)}$$

Where $\hat{\eta}$ is the theoretical response function, X_j is the coded variables of the system, and $ß_0$, $ß_j$, $ß_{jj'}$ and $ß_{jj}$ are the true model coefficients. The observed response y_i for the i_{th} experiment is y_i =

$\hat{\eta}_i + e_i$ (e_i: error).

2.2.1 The central composite design

For four variables and five levels, the total number of experiments was 31. In the present study, NO_3^- removal efficiency (%) and Q_{ad} (mg/g) were considered as the responses studied.

The coded factors using CCD is shown in Table 2. The CCD is chosen to optimize the adsorption process and to determine the regression model equations and operating parameters from the appropriate experiments. It is also an ideal design tool to find the optimum process of various factors.

The thirty-one experiments are determined by the expressions: 2^n (2^4 =8:Factor point), 2n (2×4=8 axial points) and 8 (center points: eight replications). The distance α is calculated so as to obtain rotatability. $\alpha = \pm(2^4)^{1/4} = \pm 2$.

The experimental variables X_i are coded as x_i according to the following transformation equation:

$$X_i = \frac{x_i - x_0}{\Delta x} \quad \textbf{(4)}$$

Where X_i is the uncoded value of the i^{th} independent variable and x_i is the dimensionless coded value of the i_{th} independent variable, X_0 is the value of X_i at the center point, and ΔX_i is the step change value of the real variable.

2.2.2 Validation of the model

In order to validate the model, a variance analysis study of the model is performed. Statistical analysis of the probability value according to the alpha risk is carried out to compare the experimental value with the theoretical value F (Fisher-Snedecor table).

3. Results and discussion

3.1 Effect of variables on Q_{ads} and efficiency

Several factors such as pH, mass of activated carbon, contact time, and initial nitrate concentration influence the adsorption process of NO_3^-. By applying RSM, it is possible to optimize the controllable experimental factors and to evaluate the interactions of these parameters with a limited number of experiments. The initial nitrate concentration varies between 5 and 25 mg/L. The mass of activated carbon is between 15 and 25 mg. The initial pH scale studied ranges between 3 and 7 and the contact time is between 40 and 100 min. The results included in Figure 2 shows that the adsorbed quantity of nitrate increases and becomes stable when the initial concentration of NO_3^- increases. When the contentration of ion in the solution increases, the amount adsorbed on the activated carbon increases too. As the ion diffuses into the structure of the activated carbon, the number of pores for adsorption decreases. Consequentely, the increase in percentage removal may be due to the complete utilization of all active sites in the carbon adsorbent by nitrate anions. Furthermore, as shown in Figure 2, the amount adsorbed of nitrate decreases with the increase in the mass of adsorbent. At lower pH (pH < 5) the quantity adsorbed of ion nitrate increases, then increases with the pH. In the same way, the amount of NO_3^- increases with the increase of contact time and remains constant after 70 minutes as shown in Figure 2. Moreover, the results summarized in this figure shows the relationship between nitrate adsorption rate (mg/g) and

contact time for activated carbon. The figure also demonstrates that optimal pH is equal to 4 and contact time is equal to 70 minute for this absorbent.

The main effects of each parameter on removal effeciency of NO_3^- are given in Figure 2. It was observed that the optimum current initial concentration, pH of solution, and the contact time were near 15 mg/L, 4 and 70 minutes, respectively. Removal efficiency is independent of mass of adsorbent as shown in Figure 2. The adsorption process is rapid in the first 60 min and removal efficiency is high at pH = 4, as it will decline for higher pH. Actually, the increase uptake of nitrates anions onto activated carbon for low pH ($pH \leq 4$) is due to the electrostatic interactions between the positive surface charge of activated carbon and the negative charge of nitrates. However, the adsorption of nitrates on activated carbon is carried out at different initial concentration of nitrate concentrations ranging from 5 to 25 mg/L. The evolution of the removal efficiency of NO_3^- as a function of the initial concentration of nitrates is summarized in Figure 2. The efficiency of elimination of these anions increases from the initial concentration up to 15 mg/L then gradually decreases with the increase of concentration. This result is attributed to the availability of a large number of vacant sites initially for adsorption and the presence of high surface area of activated carbon, later because of the saturation of the pores, the removal efficiency decreases. Furthermore, as seen in Figure 2, increases in mass of adsorbent have no effect on the removal effeciency of NO_3^-.

3.2 The second-order model and analysis of variance (ANOVA)

As seen in Table 4, CCD is composed of two responses Y (adsorbed amount of NO_3^- (Y_1), and % removal efficiency of NO_3^- (Y_2)). Moreover, all the 31 experimental results of adsorption capacity and the removal efficiency of nitrate anions are included in Tables 2 and 4. The regression

equations given in equations 5 and 6 are obtained after the analysis of variance in terms of coded variables gives the Q_{ads} and efficiency removal:

$$\eta_{qads} = 5.1228571 - 1.1216667\ X_1 - 0.8775\ X_2 - 0.645\ X_3 - 0.14666\ X_4 + 0.1687\ X_1X_2 - 1.0375\ X_1X_3 + 0.24375\ X_2X_3 - 0.7175\ X_1X_4 + 0.35125\ X_2X_4 - 0.1425\ X_3X_4 - 0.474048\ X_1X_1 + 0.1884524\ X_2X_2 - 0.416548\ X_3X_3 - 0.284048\ X_4X_4 \quad \textbf{(5)}$$

$$\eta_{EFF} = 85.437143 - 0.8225\ X_1 - 0.524167\ X_2 - 6.874167\ X_3 + 6.1758333\ X_4 + 7.385\ X_1X_2 - 15.0325\ X_1X_3 + 2.26875\ X_2X_3 - 13.65875\ X_1X_4 + 6.265\ X_2X_4 - 2.715\ X_3X_4 - 8.651994\ X_1X_1 + 0.361756\ X_2X_2 - 6.460744\ X_3X_3 - 4.359494\ X_4X_4 \quad \textbf{(6)}$$

The coefficients constituting the models corresponding to Equations 5 and 6 are reported in Tables 5 and 6. In order to infer the quadratic and interaction effect of the parameters, analyses are done by means of Fisher's 'F' test and Student 't' test. This means that the significant variables can be determinated based on the F value or P value. Normally, the low probability P value (also named "Prob. > |t|" value) and correspondingly the larger the magnitude of F value, the more significant is the corresponding coefficient. The results of second-order response surface model in the form of regression coefficient, F and P values for the separation factor and interaction effect of parameters are given in Tables 5 and 6 for the two responses Y_1 and Y_2. The P values are used to check the significance of each of the parameters. Values of "Prob. > |t|" greater than 0.05 indicate the model terms are not significant. As seen in table 5, P value (Prob. > |t|) is very low (less than 0.0001) of all the variables initial concentration of NO_3^-, mass of adsorbent and pH, implying that these factors

are highly significant. Moreover, all interaction effect of the factors are considered as highly significant variables except the interaction between initial concentration and mass of adsorbent (P = 0.2086) and the interaction between pH and contact time (P = 0.2849). However, it can be seen from Table 6 that for the removal efficiency of nitrate anions the P value of factors pH and contact time is low except in initial concentration (0.6752). The mass of adsorbent (0.7891) is greater than 0.1. That indicates that the pH and contact time are significant. Although, the values of "Prob. > |t| " of the whole interactions of variables are less than 0.1, implying that most of these interactions are significant except the interaction mass of adsorbent-pH (0.3506) and the interaction between pH-contact time (0.2668), which are less significant.

In order to ensure the adequacy of the used model and the tested statistical significance of the ratio of mean square variation due to regression and mean square residual error, ANOVA is used.

The P value is used as a tool to estimate if $F_{statistics}$ is large enough to indicate that most of the variation in the response can be explained by the regression model. In general, the high $F_{statistics}$ value represents high significance of the regression equation. The precision of a model can be checked by the determination coefficient (R^2). The R^2 values for percentage removal and adsorbed quantity of nitrates are 0.96 and 0.91 respectively, which is close to 1. This means that 96% and 91% of sample variation are attributed to the independent variables and only 4% and 9% of the total variation cannot be explained by the empirical model. Hence, the lower P-value and the higher value of R^2 obtained in this study for these response variables indicate that the second-order polynomial models (Eqs. (5) and (6)) are highly significant and adequate to represent the actual relationship between the response and variables. Therfore, the response surface model developed in the present study for removal efficiency and adsorbed amount of NO_3^- is good.

In order to pre-classify the influencing variables and to study the effect of interaction between variables onto adsorption process of nitrates, the graphical representation is illustrated by PARETTO diagram (Figures 3 and 4). Considering the confidence interval of the values of the coefficients (delimited by the two vertical dashed lines), it can be stated that 60% has a negatif effect on the adsorption efficiency and adsorption capacity of NO_3^-.

The analysis of the results obtained makes it possible to distinguish among the 14 coefficients studied. Three of them that appear to be highly influential onto response Y_1 (adsorption capacity q_{ads}), namely (see Figure 3) : i) Initial concentration (positive effect), ii) Mass of adsorbent (negative effect), iii) Interaction between initial concentration and pH. Three parameters that appear much less influential are : i) Interaction of initial concentration-mass of adsorbent (positive effect), ii) Contact time (positive effect), iii) Interaction between pH and contact time (negative effect).

However, it can be seen from Figure 4 (surface 2D response 2) the main effect of interaction of initial concentration-pH and the interaction between initial concentration and contact time are similarly negatively significant : i) Interaction of initial concentration-mass of adsorbent (positive effect), ii) Contact time (positive effect) , iii) Quantity adsorbed (q_{ads}).

3.3 Validation of the model

The experimental and predicted plots for percentage removal and adsorbed quantity of NO_3^- ions by adsorption onto activated carbon are shown in Figure 5. The value of R^2 is 0.91 for percentage removal as well as 0.96 for adsorbed quantity of NO_3^- ions. From the results included in Figure 4 we can see a high correlation between the experimental values and the predicted values for the adsorbed amount of NO_3^-. Further, Figure 5 reveals the predicted response values of removal efficiency of nitrate anions are in accord with the experimental values, which indicates that there are

tendencies in the linear regression fit, and the models proposed explain the experimental range studied adequately. However, the fitted regression equations show a good fit of the model.

3.4 Response surface (contour) plots and optimization conditions

Three-dimensional (3D) and contour (2D) plots for response surface are used to assess the relative effect of any two factors when the other remaining factors are held constant. Based on the regression equation, these representations are formed in order to understand the effects of variables onto responses and also to assess the change of the response surface. This means that the plots are derived from the quadratic models of Eqs (5) and (6).

The interaction effect of process variables for removal efficiency and adsorbed quantity of NO_3^- by adsorption are visualized through three dimensional views of response surface plots and are shown in Figure 6. The combined effect of initial concentration and mass of adsorbent on percentage removal and adsorbed amount of NO_3^- by adsorption process is shown in Figure 6, respectively. Thus, the surface and contour plots for removal efficiency of NO_3^- in Figure 6 shows the interaction effect of initial concentration of nitrates and mass of adsorbent at fixed values of the contact time (time = 70 min) and of the pH (pH = 4). This result shows that the response surface has a maximum point. Thereby, this contour plot indicates an increase in removal efficiency of nitrate in low concentration of nitrates value between 14 and 16 mg/L. To the contrary, working at low mass of adsorbent did not significantly affect the removal effeciency.

Graphical 3D and 2D representations of the relationships between the dependent response (adsorbed quantity of NO_3^-) and independent variables initial concentration and mass of adsorbent are presented in Figure 6. The relative effects of two variables (initial concentration of NO_3^- and mass of activated carbon) when pH value and contact time are kept constant are also included in

Figure 6. As shown in these Figure, the increase in initial concentration of NO_3^- and the decrease in mass of adsorbent increases adsorbed capacity of nitrates.These representations demonstrate that the influence of mass of adsorbent is not significant. Although, when the initial concentration of NO_3^- increases the adsorption capacity of NO_3^- increases.

The main objective of the optimization is to determine the optimum values of variables for removal efficiency of nitrate by adsorption process from the model obtained using experimental data. The optimization results of the process variables for complete removal of nitrate anions are shown in Table 7. As seen from the results included in the table, adsorption is an applicable technique for the complete removal of nitrates under reasonable operating conditions.

The optimum values of the process variables for the maximum removal efficiency of nitrates anions are shown in Table. These results demonstrate that the response surface methodology (RSM) is a powerful method for optimizing the operational conditions of the adsorption process to remove NO_3^- (Figure 7).

4. Conclusions

This study demonstrates that the elimination of nitrate ions, by adsorption on activated carbon, is effective in low nitrate concentrations. Further, it showed that response surface methodology (RSM), represented in the central composite rotatable design, is one of the suitable methods to optimize the operating conditions and maximize nitrate removal. Analysis of variance shows a high coefficient of determination value ($R^2 > 0.90$), thus ensuring a satisfactory adjustment of the second-order regression model with the experimental data. The optimization of the models provides the optimum conditions at an initial pH = 4, 15 mg/L of initial concentration of NO_3^-, and 70 min of contact time. Graphical response surface and contour plots are used to locate the optimum

point. Satisfactory prediction equation is derived for removal of nitrate using RSM to optimize the parameters.

Acknowledgment

The authors are grateful to the MOROCCAN MESRSFC. Financial Support from University Hassan II of Casablanca is also acknowledged. AG thanks Santander Bank for funding through the Research Intensification Program.

References

Acharya S, Sharma S K, Chauhan G, Shree D. 2017. Statistical Optimization of Electrocoagulation Process for Removal of Nitrates Using Response Surface Methodology, Indian Chemical Engineer. 60: 1-15.

Aguilar L, Gallegos A, Arias C A, Ferrera I, Sánchez O, Rubio R, Ben Saad M, Missagia B, Caro P, Sahuquillo S, Pérez C , Morató J. 2019. Microbial nitrate removal efficiency in groundwater polluted from agricultural activities with hybrid cork treatment wetlands, Science of the Total Environement. 653: 723-734.

Ahmadi M, Rahmani H, Ramavandi B, Kakavandi B. 2017. Removal of nitrate from aqueous solution using activated carbon modified with Fenton reagents, Desalination and Water Treatement. 76:265-275.

Ansari M H, Parsa J B, Arjomandi J. 2017. Application of conducting polyaniline, o-anisidine, o-phenetidine and o-chloroaniline in removal of nitrate from water via electrically switching ion exchange: Modeling and optimization using a response surface methodology, Separation and Purification Technology. 179:104-117.

Archin S, Sharifi S H, Asadpour. 2019. Optimization and modeling of simultaneous ultrasound-assisted adsorption of binary dyes using activated carbon from tobacco residues: Response surface methodology, Journal of Cleaner Production. 239: 118136.

Belkada F D , Kitous O , Drouiche N, Aoudj S , Bouchelaghem O, Abdi N , Grib H , Mameri N. 2018. Electrodialysis for fluoride and nitrate removal from synthesized photovoltaic industry wastewater, Separation and Purification Technology. 204: 108-115.

Dasgupta A, Matos J, Muramatsu H, Ono Y, Gonzalez V, Liu H, Rotella C, Fujisawa K, Cruz-Silva R, Hashimoto Y, Endo M, Kaneko K, Radovic L R, Terrrones M. 2018. Nanostructured carbon materials for enhanced nitrobenzene adsorption: Physical vs. chemical surface properties, Carbon. 139:833-844.

Dražević E, Košutić K, Svalina M, Catalano J. 2017. Permeability of uncharged organic molecules in reverse osmosis desalination membranes, Water Res.116:13-22.

El Hanache L, Sundermann L , Lebeaua B, Toufaily J, Hamieh T, Daoua T J. 2019. Surfactant-modified MFI-type nanozeolites: Super-adsorbents for nitrate removal from contaminated water. Microporous and Mesoporous Materials. 283:1-13.

El Mouzdahir Y, Elmchaouri A, Mahboub R, ElAnssari A, Gil A, Korili S A, Vicente MA. 2007. Interaction of stevensite with Cd^{2+} and Pb^{2+} in aqueous dispersions, Applied Clay Science. 37: 47-58.

Epsztein R, Nir O, Lahav O, Green M. 2015. Selective nitrate removal from groundwater using a hybrid nanofiltration–reverse osmosis filtration scheme, Chemical Engineering Journal. 279:372-378.

Fan C, Zhang Y. 2018. Adsorption isotherms, kinetics and thermodynamics of nitrate and phosphate in binary systems on a novel adsorbent derived from corn stalks, Journal of Geochemical Exploration. 188:95-100.

Fu F, Dioysiou D D, Liu H. 2014. The use of zero-valent iron for groundwater remediation and wastewater treatment: A review, Journal of Hazardous Materials. 267: 194-205.

García-Fernández M J , Pastor-Blas M M , Epron F, Sepúlveda-Escribano A. 2018. Proposed mechanisms for the removal of nitrate from water by platinum catalysts supported on polyaniline and polypyrrole, Applied Catalysis B: Environmental. 225: 162-171.

Ghasemi M, Mashhadi S, Asif M, Tyagi I, Agarwal S, Gupta V K. 2016. Microwaveassisted synthesis of tetraethylenepentamine functionalized activated carbon with high adsorption capacity for Malachite green dye, J. Mol. Liq. 213:317–325.

Golie W M and Upadhyayula S.2017. An investigation on biosorption of nitrate from water by chitosan based organic-inorganic hybrid biocomposites, International Journal of Biological Macromolecules. 97: 489-502.

Gouran-Orimi R, Mirzayi B, Nematollahzadeh A, Tardast A. 2018. Competitive Adsorption of Nitrate in Fixed-Bed Column Packed with Bio-inspired Polydopamine Coated Zeolite, Journal of Environmental Chemical Engineering. 6: 2232-2240.

Gadekar M R. Ahammed M. 2019. Modelling dye removal by adsorption onto water treatment residuals using combined response surface methodology-artificial neural network approach, Journal of Environmental Management. 231: 241-248.

Hanafi H A and Azeema S M A. 2016. Removal of nitrate and nitrite anions from wastewater using activated carbon derived from rice straw. J Environ Anal Toxicol 6: 346.

Karri R R, Sahu J N, Chimmiri V. 2018. Critical review of abatement of ammonia from wastewater, Journal of Molecular liquids. 261:21-31.

Kalantary R R, Dehghanifard E, Mohseni-Bandpi A, Razaei L, Esrafili A, Kakavandi B, Azari A. (2016) Nitrate adsorption by synthetic activated carbon magnetic nanoparticles: kinetics, isotherms and thermodynamic studies. Desalination and Water Treatment 57: 16445-16455.

Karamati-Niaragh E, Moghaddam M R A, Emamjomeh M M, Nazlabadi E. 2019. Evaluation of direct and alternating current on nitrate removal using a continuous electrocoagulation process: Economical and environmental approaches through RSM, Journal of Environmental Management. 230:245-254.

Kuang P, Chen N, Feng C, Li M, Dong S , Lv L, Zhang J, Hu Z, Deng Y. 2018. Construction and optimization of an iron particle–zeolite packing electrochemical–adsorption system for the simultaneous removal of nitrate and by-products, Journal of the Taiwan Instiyute of Chemical Engineers. 86:101-112.

Li E, Wang R, Jin X, Lu S, Qiu Z, Zhang X. 2018. Investigation into the nitrate removal efficiency and microbial communities in a sequencing batch reactor treating reverse osmosis concentrate produced by a coking wastewater treatment plant, Environmental Technology. 39: 1-43.

Li P, Lin K, Fang Z, Wang K. 2017. Enhanced nitrate removal by novel bimetallic Fe/Ni nanoparticles supported on biochar, Journal of Cleaner Production. 151:21-33.

Lu J S, Lian T t, Su J f. 2018. Effect of zero-valent iron on biological denitrification in the autotrophic denitrification system, Res Chem Intermed. 44: 6011-6022.

Luo W, Phan H V, Xie M, Hai F I, Price W E, Elimelech M, Nghiem L D. 2017. Osmotic versus conventional membrane bioreactors integrated with reverse osmosis for water reuse: Biological stability, membrane fouling, and contaminant removal, Water Res, 109:122-134.

Mankiewicz-Boczek J, Bednarek A, Gagała-Borowska I, Serwecinska L, Zaborowski A, Kolate E, Pawełczyk J, Zaczek A, Dziadek J, Zalewski M. 2017. The removal of nitrogen compounds from farming wastewater – The effect of different carbon substrates and different microbial activators, Ecological Engineering. 105:341-354.

Mazarji M, Aminzadeh B, Baghdadi M, Bhatnagar A. 2017. Removal of nitrate from aqueous solution using modified granular activated carbon, Journal of Molecular Liquids. 233: 139-148.

Moreira M A, Ciuffi K J, Rives V, Vicente M A, Trujillano R, Gil A, Korili S A, de Faria E H. 2017. Effect of chemical modification of palygorskite and sepiolite by 3-

aminopropyltriethoxisilane on adsorption of cationic and anionic dyes, Applied Clay Science. 135: 394-404.

Mubita T M, Dykstra J E, Biesheuvel P M, van der Wal A, Porada S. 2019. Selective adsorption of nitrate over chloride in microporous carbons, Water Research.164: 114885.

Onorato C, Banasiak L J, Schafer A I. 2017. Inorganic trace contaminant removal from real brackish groundwater using electrodialysis, Separation and Purification Technology. 187: 426-435.

Piai L, Dykstra J E, Adishakti M G, Blokland M, Langenhoff A A M, van der Wal A. 2019. Diffusion of hydrophilic organic micropollutants in granular activated carbon with different pore sizes, Water Research. 162:518-527.

Pirsaheb M , Khosravi T , Sharafi K, Mouradi M. 2016. Comparing operational cost and performance evaluation of electrodialysis and reverse osmosis systems in nitrate removal from drinking water in Golshahr, Mashhad, Desalination and Water Treatment. 57: 1-7.

Sabeti M B, Hejazi M A, Karimi A. 2019. Enhanced removal of nitrate and phosphate from wastewater by Chlorella vulgaris: Multi-objective optimization and CFD simulation,Chinese Journal of Chemical Engineering. 27:639-648.

Sanctis M D, Moro G D, Chimienti S, Ritelli P, Levantesi C, Laconi C D. 2017. Removal of pollutants and pathogens by a simplified treatment scheme for municipal wastewater reuse in agriculture, Science of the Total Environment. 580: 17-25.

Satayeva A R, Howell C A, Korobeinyk A V, Jandosov J, Inglezakis V J, Mansurov Z A, Mikhalovsky S V. 2018. Investigation of rice husk derived activated carbon for removal of nitrate contamination from water, Science of the Total Environment. 630:1237-1245.

Schullehner J, Stayner L, Hansen B. 2017. Nitrate, Nitrite, and Ammonium Variability in Drinking Water Distributio Systems, Int. J. Environ. Public Health. 14:1-9.

Song M, Li M. 2019. Adsorption and regeneration characteristics of phosphorus from sludge dewatering filtrate by magnetic anion exchange resin, Environ Sci Pollut Res.

Song P, Wu L, Guan W. 2015. Dietary nitrates, nitrites, and nitrosamines intake and the risk of gastric cancer: a meta-analysis, Nutrients. 7: 9872–9895.

Su J F , Zheng S C , Huang T L, Ma F, Shao S C , Yang S F, Zhang L N. 2016. Simultaneous removal of Mn(II) and nitrate by the manganese-oxidizing bacterium Acinetobacter sp. SZ28 in anaerobic conditions. Geomicrobiology Journal, 33:1-23.

Torre U D-L, -Ayo B P, Moliner M , González-Velasco J R. 2016. Cu-zeolite catalysts for NO_x removal by selective catalytic reduction with NH_3 and coupled to NO storage/reduction monolith in diesel engine exhaust aftertreatment systems, Applied Catalysis B: Environmental. 187: 419-427.

Uzun H I, Debik E. 2019. Economical approach to nitrate removal via membrane capacitive deionization, Separationand purification Technology. 209: 776-781.

Villanueva C M, Kogevinas M, Cordier S, Templeton M R, Vermeulen R, Nuckols J R, Nieuwenhuijsen M J, Levallois P. 2014. Assessing exposure and health consequences of chemicals in drinking water: current state of knowledge and research needs, Environ Health Perspect. 122:213-221.

Wongsanit J, Teartisup P, Kerdsueb P, Tharnpoophasiam P, Worakhunpiset S. 2015. Contamination of nitrate in groundwater and its potential human health: a case study of lower Mae Klong river basin, Thailand, Environ Sci Pollut Res. 22: 11504-11512.

Yuana J, Amanob Y, Machida M. 2019. Surface modified mechanism of activated carbon fibers by thermal chemical vapor deposition and nitrate adsorption characteristics in aqueous solution. Colloids and Surfaces A. 580: 123710.

Yun Y, Li Z, Chen Y –H, Saino M, Cheng S, Zheng L. 2016. Catalytic reduction of nitrate in secondary effluent of wastewater treatement plants by Fe^0 and pd-Cu/ ϒ-Al_2O_3, Water Science & Technology. 73: 2697-2703.

Zhang B, Liu Y, Tong S, Zheng M, Zhao Y, Tian C, Liu H, Feng C. 2014. Enhancement of bacterial denitrification for nitrate removal in groundwater with electrical stimulation from microbial fuel cells, Journal of Power Sources. 268: 423-429.

Zhang W, Bai Y, Ruan X, Yin L. 2019. The biological denitrification coupled with chemical reduction for groundwater nitrate remediation via using SCCMs as carbon source, Chemosphere. 234: 89-97.

Zhang Y, Wei D, Morrison L, Ge Z, Zhan X, Li R. 2019. Nutrient removal through pyrrhotite autotrophic denitrification: Implications for eutrophication control, Science of the Total Environment. 662:287-296.

Captions:

Table 1. Chemical compositions of activated carbon by inductively coupled plasma mass spectrometry (ICP-MS).

Table 2. The Central Composite Design (CCD) for the four independent variables.

Table 3. Experimental range and levels of independent process variables.

Table 4. Experimental and theoretically predicted values for Q_{ads} and Efficiency removal of nitrate.

Table 5. Estimated regression coefficients and corresponding F and P values for adsorption capacity of NO_3^- (Q_{ads}).

Table 6. Estimated regression coefficients and corresponding F and P values for percentage removal of NO_3^-.

Table 7. Optimum values of the process parameters for maximum removal efficiency of nitrate.

Figure 1. Procedure for the adsorption on Nitrates onto Activated Carbon.

Figure 2. Main effect plots of parameters for: (a) adsorption capacity of NO_3^-, (b) removal efficiency of NO_3^-.

Figure 3. Graphical representation of the effects of factors on adsorption capacity of NO_3^-.

Figure 4. Graphical representation of the effects of factors on removal efficiency of values of the linear and quadratic coefficients of the mathematical equations expressing the variation of adsorbed quantity (Y_1) and efficiency (Y_2).

Figure 5. The predicted values (%) plotted against experimental values (%) (a) adsorbed quantity of NO_3^- (b) removal efficiency of NO_3^-. The long dash line is the regression line with regression

coefficient R 0.96 for aadsorbed quantity of nitrate and R 0.96 for removal efficiency of NO_3^-. Each point refers to the experiment number listed in Table 4.

Figure 6. Surface and contour plots of estimated response surface : (a) adsorbed capacity of nitrates, (b) removal efficiency of nitrates (Contact time=70 min, pH=4).

Figure 7. Response surface and contour Plot of removal efficiency (%) and adsorption capacity (Qads) according to the optimized parameters. pH = 4. Contact time = 70 min.

Table 1. Chemical compositions of activated carbon by inductively coupled plasma mass spectrometry (ICP-MS).

Elements	C	S	SiO_2	Al_2O_3	FeO_3	CaO	MnO	TiO_2
Pourcentage (%)	85.12	0.05	0.18	1.09	0.05	0.1	0.71	0.078

Table 2. The Central Composite Design (CCD) for the four independent variables.

Logical run	Random run	Coded variables values				Uncoded variables values				Responses values	
		X_1 C_i	X_2 Weight	X_3 pH	X_3 Contact Time	X_1 C_i	X_2 Weight	X_3 pH	X_4 Contact Time	Q_{ads}	Efficiency Removal %
1	26	-1	-1	-1	-1	20	30	6	50	2.4	48.19
2	24	-1	-1	-1	1	10	30	6	50	4.8	96.08
3	31	-1	-1	1	-1	20	20	6	90	3.95	79.16
4	18	-1	-1	1	1	15	25	5	70	4.65	93.05
5	13	-1	1	-1	-1	25	25	5	70	0.55	16.56
6	30	-1	1	-1	1	20	30	4	90	2.47	74.39
7	2	-1	1	1	-1	15	15	5	70	1.52	45.83
8	19	-1	1	1	1	15	25	5	70	3.3	99
9	16	1	-1	-1	-1	15	25	5	70	9.05	90.51
10	23	1	-1	-1	1	15	25	5	70	6.8	68.07
11	21	1	-1	1	-1	5	25	5	70	5	50
12	3	1	-1	1	1	15	25	5	70	2.4	24.05
13	27	1	1	-1	-1	10	30	4	50	5.67	85.09
14	6	1	1	-1	1	15	25	5	70	5.8	87.04
15	1	1	1	1	-1	15	25	5	70	3.24	48.64
16	28	1	1	1	1	20	20	4	50	3.28	49.32
17	11	-2	0	0	0	15	25	7	70	0.88	44.16
18	5	2	0	0	0	10	20	6	90	5.9	59.06
19	7	0	-2	0	0	10	30	6	90	8	80
20	29	0	2	0	0	15	25	5	110	4.08	95.33
21	25	0	0	-2	0	20	20	6	50	4.94	82.4
22	17	0	0	2	0	15	25	5	30	2.3	38.35
23	22	0	0	0	-2	20	20	4	90	3.8	63.48
24	20	0	0	0	2	10	20	4	90	4.5	74.08
25	4	0	0	0	0	15	25	3	70	5.87	97.97
26	8	0	0	0	0	10	20	4	50	5.44	90.74
27	9	0	0	0	0	20	30	4	50	4.33	72.22
28	10	0	0	0	0	20	30	6	90	5.22	87.03
29	12	0	0	0	0	15	35	5	70	4.8	80
30	14	0	0	0	0	10	30	4	90	5.1	85
31	15	0	0	0	0	10	20	6	50	5.1	85.1

Table 3. Experimental range and levels of independent process variables.

	Coded variables X_1 , X_2 , X_3 , X_4*					Δx
Natural variables (x_j)	-2	-1	0	1	2	
x_1= initial Concentration	5	10	15	20	25	5
x_2= weight of adsorbent (mg)	15	20	25	30	35	5
x_3= pH	3	4	5	6	7	1
x_4= Contact time (min)	30	50	70	90	110	20

*$X_1=(x_1 – 15)/5$; $X_2 = (x_2 – 25)/5$; $X_3 = (x_3 – 5)/1$ and $X_4 = (x_4 – 70)/20$

Table 4. Experimental and theoretically predicted values for Q_{ads} and Efficiency removal of nitrate.

Q_{ads} / ($mg.g^{-1}$)			Efficiency (%)		
Q_{ads} experimental	Q_{ads} predicted	Standard error	Efficiency experimental	Efficiency predicted	Standard error
2.4	3.227	-0.827	48.19	52.884	-4.694
4.8	4.538	0.262	96.08	85.453	10.627
3.95	3.81	0.14	79.16	70.093	9.067
4.65	4.55	0.1	93.05	91.803	1.248
0.55	-0.055	0.605	16.56	19.998	-3.438
2.47	2.66	-0.19	74.39	77.628	-3.238
1.52	1.502	0.018	45.83	46.283	-0.453
3.3	3.648	-0.348	99	93.052	5.948
9.05	8.703	0.347	90.51	93.852	-3.342
6.8	7.144	-0.344	68.07	71.786	-3.716
5	5.135	-0.135	50	50.931	-0.931
2.4	3.006	-0.606	24.05	18.005	6.045
5.67	6.095	-0.425	85.09	90.506	-5.416
5.8	5.941	-0.141	87.04	93.5	-6.46
3.24	3.503	-0.263	48.64	56.66	-8.02
3.28	2.779	0.501	49.32	48.794	0.526
0.88	0.923	-0.043	44.16	52.474	-8.314
5.9	5.53	0.37	59.06	49.184	9.876
8	7.632	0.368	80	87.933	-7.933
4.08	4.122	-0.042	95.33	85.836	9.494
4.94	4.747	0.193	82.4	73.343	9.058
2.3	2.167	0.133	38.35	45.846	-7.496
3.8	3.693	0.107	63.48	55.648	7.833
4.5	4.28	0.22	74.08	80.351	-6.271
5.87	5.123	0.747	97.97	85.437	12.533
5.44	5.123	0.317	90.74	85.437	5.303
4.33	5.123	-0.793	72.22	85.437	-13.217
5.22	5.123	0.097	87.03	85.437	1.593
4.8	5.123	-0.323	80	85.437	-5.437
5.1	5.123	-0.023	85	85.437	-0.437
5.1	5.123	-0.023	85.1	85.437	-0.337

Table 5. Estimated regression coefficients and corresponding F and P values for adsorption capacity of NO_3^- (Q_{ads}).

Term	Coefficient	Standard error	Sum of squares	Report F	Prob. > |t|	Significance
Constant	5.1228571	0.194698	-	-	<.0001	***
Initial concentration	1.1516667	0.105149	31.832067	119.9621	<.0001	***
Weight	-0.8775	0.105149	18.48015	69.6441	<.0001	***
pH	-0.645	0.105149	9.9846	37.6279	<.0001	***
Contact time	0.1466667	0.105149	0.516267	1.9456	0.1821	NS
Initial concentration*Weight	0.16875	0.128781	0.455625	1.7171	0.2086	NS
Initial concentration*pH	-1.0375	0.128781	17.2225	64.9046	<.0001	***
Weight*pH	0.24375	0.128781	0.950625	3.5825	0.0766	*
Initialnconcentration*Contact time	-0.7175	0.128781	8.2369	31.0415	<.0001	***
Weight*Contact time	0.35125	0.128781	1.974025	7.4393	0.0149	*
pH*Contact time	-0.1425	0.128781	0.3249	1.2244	0.2849	NS
Initial concentration*Initial concentration	-0.474048	0.09633	6.426068	24.2172	0.0002	***
Weight*Weight	0.1884524	0.09633	1.015558	3.8272	0.0681	NS
pH* pH	-0.416548	0.09633	4.961703	18.6986	0.0005	***
Contact time*Contact time	-0.284048	0.09633	2.307192	8.6949	0.0094	**

*** : significant to 0.1 % ($F_{0.001(1.16)} = 16.12$)

** : significant to 1 % ($F_{0.01(1.16)} = 8.53$)

* : significant to 5 % ($F_{0.05(1.16)} = 4.49$)

NS : not significant

Table 6. Estimated regression coefficients and corresponding F and P values for percentage removal of NO_3^-.

Term	Coefficient	Standard error	Sum of squares	Report F	Prob. > |t|	Significance
Constant	85.437143	3.567667	-	-	<.0001	***
Initial concentration(10.20)	-0.8225	1.92676	16.2361	0.1822	0.6752	NS
Weight(20.30)	-0.524167	1.92676	6.594	0.074	0.7891	NS
pH(4.6)	-6.874167	1.92676	1134.1	12.7287	0.0026	**
Contact time(50.90)	6.1758333	1.92676	915.382	10.2739	0.0055	**
Initial concentration*Weight	7.385	2.35979	872.6116	9.7939	0.0065	**
Initial concentration*pH	-15.0325	2.35979	3615.6169	40.5803	<.0001	***
Weight*pH	2.26875	2.35979	82.3556	0.9243	0.3506	NS
Initial concentration*Contact time	-13.65875	2.35979	2984.9832	33.5023	<.0001	***
Weight*Contact time	6.265	2.35979	628.0036	7.0485	0.0173	*
pH*Contact time	-2.715	2.35979	117.9396	1.3237	0.2668	NS
Initial concentration* Initial concentration	-8.651994	1.765154	2140.5917	24.0252	0.0002	***
Weight*Weight	0.361756	1.765154	3.7422	0.042	0.8402	NS
pH*pH	-6.460744	1.765154	1193.6211	13.3968	0.0021	**
Contact time*Contact time	-4.359494	1.765154	543.4675	6.0997	0.0252	*

*** : significant to 0.1 % (F0.001(1.16) = 16.12)

** : significant to 1 % (F0.01(1.16) = 8.53)

* : significant to 5 % (F0.05(1.16) = 4.49)

NS : not significant

Table 7. Optimum values of the process parameters for maximum removal efficiency of nitrate anions.

Parameter	Experimental value
X_1=Initial concentration(mg.L^{-1})	15
X_2=Mass of Adsorbent (mg)	25
X_3=pH	4
X_4=Contact Time (min)	70

.

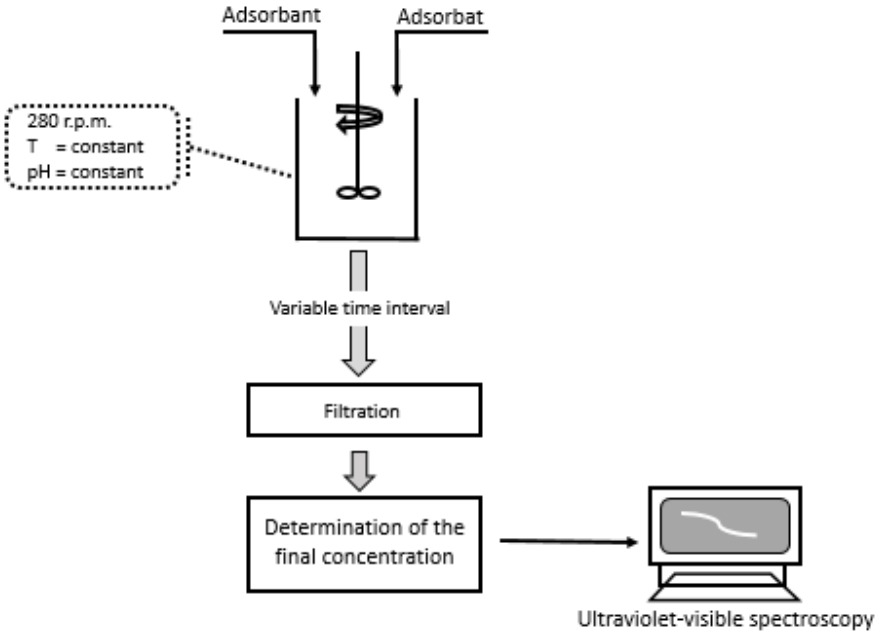

Figure 1. Procedure for the adsorption on Nitrates onto Activated Carbon.

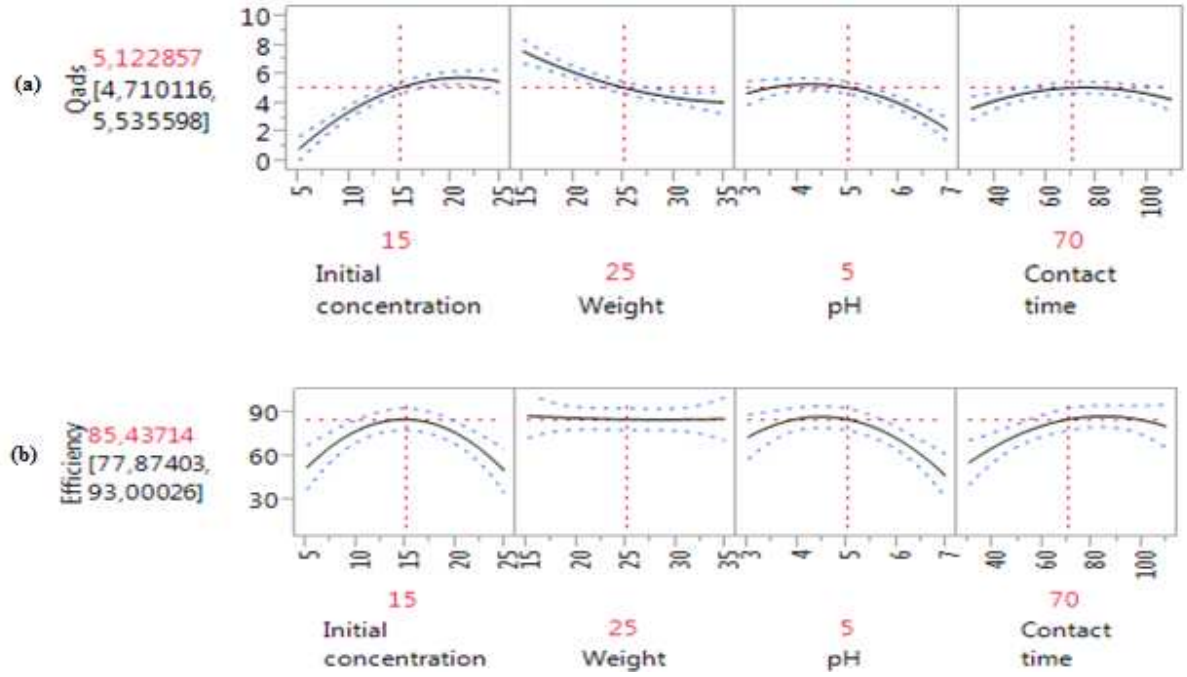

Figure 2. Main effect plots of parameters for: (a) adsorption capacity of NO_3^-, (b) removal efficiency of NO_3^-.

Term	Coefficient	Pareto diagram	Prob. > |t|
Initial concentration(10,20)	1.1516667	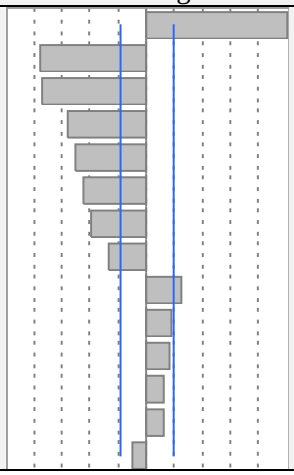	<.0001*
Weight(20,30)	-0.8775		<.0001*
Initial concentration*pH	-1.0375		<.0001*
pH(4,6)	-0.645		<.0001*
Initial concentration*Contact time	-0.7175		<.0001*
Initial concentration* Initial concentration	-0.474048		0.0002*
pH*pH	-0.416548		0.0005*
Contact time*Contact time	-0.284048		0.0094*
Weight*Contact time	0.35125		0.0149*
Weight*Weight	0.1884524		0.0681
Weight*pH	0.24375		0.0766
Contact time(50,90)	0.1466667		0.1821
Initial concentration*Weight	0.16875		0.2086
pH*Contact time	-0.1425		0.2849

Figure 3. Graphical representation of the effects of factors on adsorption capacity of NO_3^-.

Terme	Estimation	t ratio	Prob. > |t|
Initial concentration*pH	-15.0325	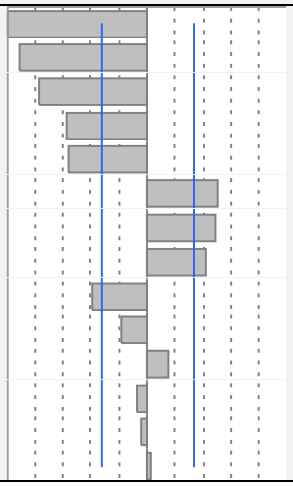	<.0001*
Initial concentration*Contact time	-13.65875		<.0001*
Initial concentration* Initial concentration	-8.651994		0.0002*
pH*pH	-6.460744		0.0021*
pH(4.6)	-6.874167		0.0026*
Contact time(50.90)	6.1758333		0.0055*
Initial concentration*Weight	7.385		0.0065*
Weight*Contact time	6.265		0.0173*
Contact time*Contact time	-4.359494		0.0252*
pH*Contact time	-2.715		0.2668
Weight*pH	2.26875		0.3506
Initial concentration(10.20)	-0.8225		0.6752
Weight(20.30)	-0.524167		0.7891
Weight*Weight	0.361756		0.8402

Figure 4. Graphical representation of the effects of factors on removal efficiency of values of the linear and quadratic coefficients of the mathematical equations expressing the variation of adsorbed quantity (Y_1) and efficiency (Y_2).

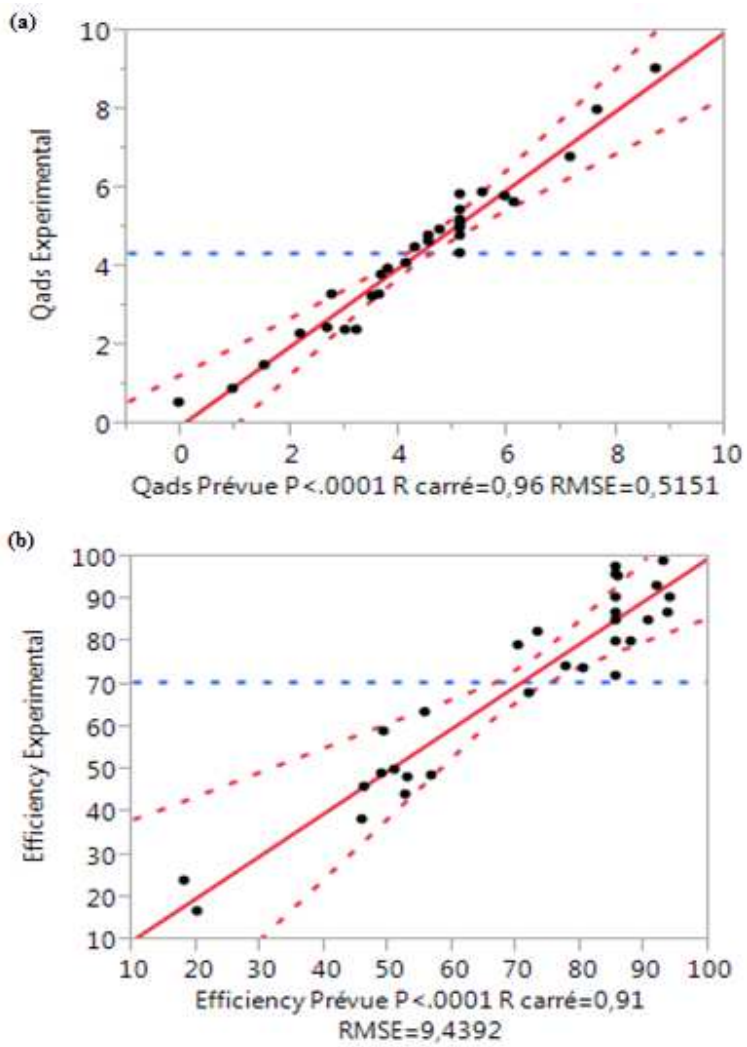

Figure 5. The predicted values (%) plotted against experimental values (%) (a) adsorbed quantity of NO_3^- (b) removal efficiency of NO_3^-. The long dash line is the regression line with regression coefficient R 0.96 for aadsorbed quantity of nitrate and R 0.96 for removal efficiency of NO_3^-. Each point refers to the experiment number listed in Table 4.

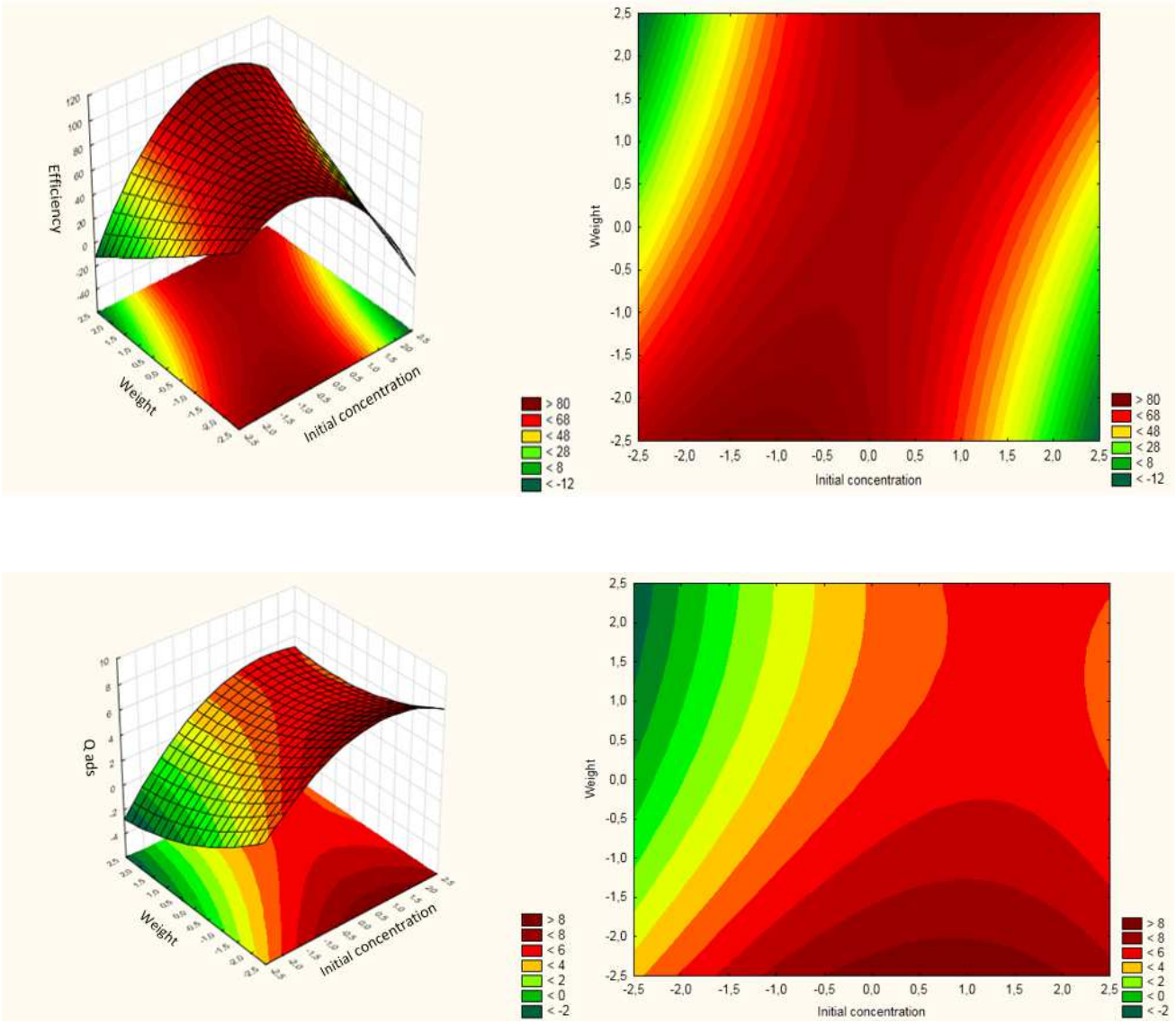

Figure 6. Surface and contour plots of estimated response surface : (a) adsorbed capacity of nitrates, (b) removal efficiency of nitrates (Contact time=70 min, pH=4).

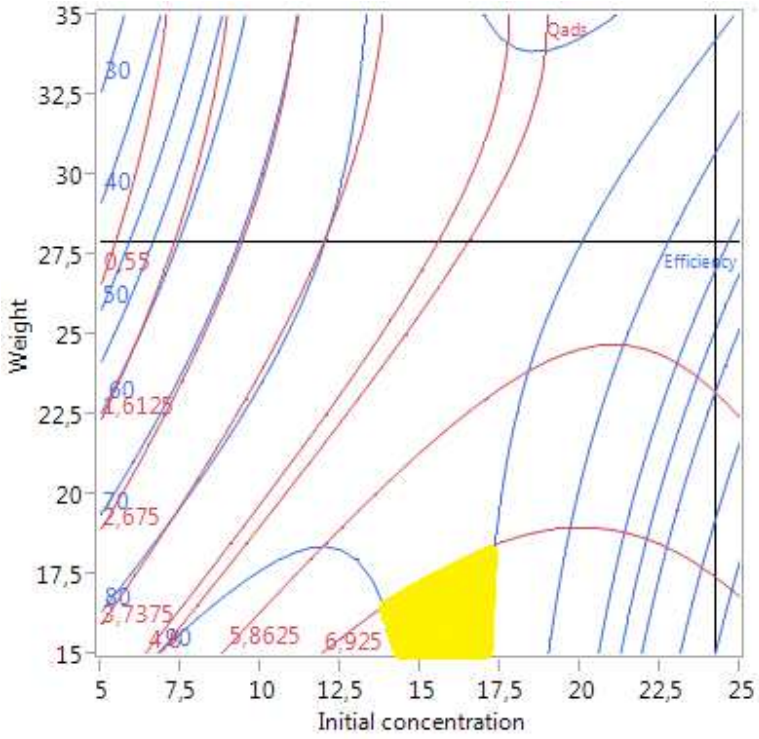

Figure 7. Response surface and contour Plot of removal efficiency (%) and adsorption capacity (Q_{ads}) according to the optimized parameters. pH = 4. Contact time = 70 min.